Generating end modes in a superconducting wire by periodic driving of the hopping

Siddhartha Saha,[1] Shankar N. Sivarajan,[1] and Diptiman Sen[2]
[1]*Undergraduate Programme, Indian Institute of Science, Bengaluru 560 012, India*
[2]*Centre for High Energy Physics, Indian Institute of Science, Bengaluru 560 012, India*
(Received 26 October 2016; published 31 May 2017)

We show that harmonic driving of either the magnitude or the phase of the nearest-neighbor hopping amplitude in a p-wave superconducting wire can generate modes localized near the ends of the wire. The Floquet eigenvalues of these modes can either be equal to ± 1 (which is known to occur in other models) or can lie near other values in complex conjugate pairs, which is unusual; we call the latter anomalous end modes. All the end modes have equal probabilities of particles and holes. If the amplitude of driving is small, we observe an interesting bulk-boundary correspondence for the anomalous end modes: the Floquet eigenvalues and the peaks of the Fourier transform of these end modes lie close to the Floquet eigenvalues and momenta at which the Floquet eigenvalues of the bulk system have extrema.

DOI: 10.1103/PhysRevB.95.174306

I. INTRODUCTION

The last several years have witnessed extensive studies of topological phases of matter [1–3]. A system in a topological phase has only gapped states in the bulk but has gapless states at the boundaries. In addition, the number of gapless boundary modes is given by a topological invariant which depends on the properties of the bulk and its symmetries such as time-reversal and particle-hole symmetry. Such a relation between the properties of the bulk and the boundary modes is called a bulk-boundary correspondence.

Recently, there have been several studies of systems in which the Hamiltonian is varied in time in a periodic way leading to some topological features such as the generation of boundary modes [4–35]. Some of these topological aspects have been experimentally studied [36–41]. However, the existence of topological invariants and the relation between them and the number of boundary modes is not always clear. Further, in many models, the boundary modes turn out to be of only two types corresponding to eigenvalues of the Floquet operator being $+1$ or -1. It would be interesting to know if this is always the case. In this paper, we examine some of these questions for a one-dimensional model where the end modes and topological invariants can be numerically studied relatively easily.

The plan of this paper is as follows. In Sec. II we introduce the system of interest. We will consider a lattice model of spinless electrons with p-wave superconducting pairing; this is sometimes called the Kitaev chain [42]. We will review the energy spectrum and the different phases (topological and non-topological) that this model has when the Hamiltonian is time independent. The phase diagram is known to change in an interesting way if the hopping amplitude is allowed to be complex; we get regions in parameter space where the bulk spectrum is gapless [43]. We present two topological invariants which one-dimensional models with and without time-reversal symmetry have when periodic boundary conditions are imposed. In Sec. III, we discuss in general how we can numerically study the Floquet time evolution and the modes which appear at the ends of a system when the Hamiltonian varies periodically with time. In Sec. IV, we study what happens when the phase or magnitude of the hopping is driven harmonically in time. We study the ranges of parameters in which modes appear at the ends of an open chain and various properties of these modes such as their number and Floquet eigenvalues. We find that the Floquet eigenvalues can be equal to either ± 1 or any other complex number with unit magnitude; in the latter case they have to appear in complex conjugate pairs, and we call these anomalous end modes. We calculate the Fourier transforms of the wave functions of the end modes and find that they have peaks at certain values of k; in particular, the Fourier transforms of the anomalous end modes have peaks at zero and π. The expectation value of the electron number is found to be zero in all the end modes; hence they have equal probabilities of particles and holes. We find that the anomalous end modes disappear when the chemical potential is moved sufficiently away from zero. In Sec. V we examine if there are any bulk-boundary correspondences in this periodically driven system. We first examine a topological invariant called the winding number and find that it matches the number of modes at each end of the chain which have Floquet eigenvalues equal to 1 for the case that the magnitude of the hopping is periodically driven but not in the case that the phase of the hopping is driven. A corresponding topological invariant for the anomalous end modes does not seem to exist. When the amplitude of the periodic driving is small, we find a different kind of bulk-boundary correspondence which works for all the anomalous end modes. Namely, if we look at the Floquet eigenvalues of the bulk system as a function of the momentum k, we find that the values of k where these eigenvalues have extrema and the corresponding Floquet eigenvalues match closely the values of k where the Fourier transforms of the wave functions of the anomalous end modes have peaks and the Floquet eigenvalues of those end modes. In Sec. VI, we use a Floquet-Magnus expansion to study the system when the driving frequency is much larger than the other energy scales like the hopping and the superconducting pairing. In this limit, we find that the number of end modes is the same as that found when there is no driving. We summarize our main results and point out possible directions for future studies in Sec. VII.

II. KITAEV CHAIN

In this section, we will review the properties of the Kitaev chain, its phase diagram, and topological invariants. The Kitaev chain is a model of spinless electrons on a lattice with a nearest-neighbor hopping amplitude γ, a p-wave

superconducting pairing Δ between neighboring sites, and a chemical potential μ. For a finite and open chain with N sites, the Hamiltonian takes the form

$$H = \sum_{n=1}^{N-1}[\gamma f_n^\dagger f_{n+1} + \gamma^* f_{n+1}^\dagger f_n + \Delta(f_n f_{n+1} + f_{n+1}^\dagger f_n^\dagger)] - \sum_{n=1}^{N} \mu f_n^\dagger f_n, \quad (1)$$

where Δ and μ are real, but γ may be complex. We write the hopping as

$$\gamma = \gamma_0 e^{i\phi}, \quad (2)$$

where γ_0 is real and positive. We will assume that all these parameters are time independent in this section. The operators f_n in Eq. (1) satisfy the anticommutation relations $\{f_m, f_n\} = 0$ and $\{f_m, f_n^\dagger\} = \delta_{mn}$. (We will set both Planck's constant $\hbar$ and the lattice spacing equal to 1 in this paper). We introduce the Majorana operators

$$b_{2n-1} = f_n + f_n^\dagger \quad \text{and} \quad b_{2n} = i(f_n - f_n^\dagger), \quad (3)$$

for $n = 1,2,\ldots,N$. It is easy to check that these are Hermitian operators satisfying $\{b_m,b_n\} = 2\delta_{mn}$. In terms of these operators, Eq. (1) takes the form

$$H = \frac{i}{2}\sum_{n=1}^{N-1}[(\gamma_0\cos\phi - \Delta)b_{2n}b_{2n+1} - (\gamma_0\cos\phi + \Delta) \times b_{2n-1}b_{2n+2} + \gamma_0 \sin\phi(b_{2n-1}b_{2n+1} + b_{2n}b_{2n+2})] + \frac{i}{2}\sum_{n=1}^{N}\mu b_{2n-1}b_{2n}, \quad (4)$$

up to a constant. Note that the Hamiltonian is invariant under the parity transformation $\mathcal{P}$ corresponding to a reflection of the system about its midpoint, i.e., $b_{2n} \to (-1)^n b_{2N+1-2n}$ and $b_{2n+1} \to b_{2N-2n}$.

The Hamiltonian in Eq. (4) has a time-reversal symmetry if γ is real, i.e., if $\phi = 0$ or π. The time-reversal transformation involves complex conjugating all numbers, including $i \to -i$, and

$$b_{2n} \to -b_{2n} \quad \text{and} \quad b_{2n+1} \to b_{2n+1}. \quad (5)$$

Note that f_n and $f_n^\dagger$ remain invariant under this transformation; this implies that their Fourier transforms (defined below) transform as $f_k \to f_{-k}$ and $f_k^\dagger \to f_{-k}^\dagger$.

The Hamiltonian in Eq. (4) has particle-hole symmetry if $\mu = 0$. The particle-hole symmetry transforms $f_n \to (-1)^n f_n^\dagger$, namely,

$$b_{2n-1} \to (-1)^n b_{2n-1} \quad \text{and} \quad b_{2n} \to -(-1)^n b_{2n}, \quad (6)$$

and complex conjugates all numbers including $\gamma \to \gamma^*$.

It is convenient to define an operator

$$F = \sum_{n=1}^{N}(2f_n^\dagger f_n - 1) = -i\sum_{n=1}^{N} b_{2n-1}b_{2n}. \quad (7)$$

This is related to the total electron number, $\sum_n f_n^\dagger f_n$, by some constants. We will see later how F can be used to calculate the average electron number of the end modes.

The energy spectrum of Eq. (4) in the bulk can be found by considering a chain with periodic boundary conditions. We define the Fourier transform $f_k = \frac{1}{\sqrt{N}}\sum_{n=1}^{N} f_n e^{ikn}$, where the momentum k goes from $-\pi$ to π in steps of $2\pi/N$. Then Eq. (1) can be written in momentum space as

$$H = \sum_{0\leqslant k\leqslant\pi} \begin{pmatrix} f_k^\dagger & f_{-k} \end{pmatrix} h_k \begin{pmatrix} f_k \\ f_{-k}^\dagger \end{pmatrix}, \quad (8)$$

$$h_k = 2\gamma_0 \sin\phi \sin k I_2 + (2\gamma_0\cos\phi\cos k - \mu)\tau^z + 2\Delta \sin k \tau^y, \quad (9)$$

where I_2 denotes the two-dimensional identity matrix and the τ^a's are Pauli matrices. The dispersion relation follows from Eqs. (8) and (9) and is given by [43]

$$E_{k\pm} = 2\gamma_0 \sin\phi \sin k \pm \sqrt{(2\gamma_0\cos\phi\cos k - \mu)^2 + 4\Delta^2 \sin^2 k}. \quad (10)$$

Depending on the values of γ_0, ϕ, Δ, and μ, the system has four phases where E_k is nonzero for all values of k, i.e., the bulk spectrum is gapped [43]. The phase diagram is shown in Fig. 1. Phase I lies in the region $\Delta/\gamma_0 > \sin\phi$ and $-2\cos\phi < \mu/\gamma_0 < 2\cos\phi$, while phase II lies in the region $\Delta/\gamma_0 < -\sin\phi$ and $-2\cos\phi < \mu/\gamma_0 < 2\cos\phi$. In these two phases, a long and open chain has a zero energy mode at each end; hence these are called topological phases. Phases III and IV are nontopological phases in which there are no end modes. In addition to these phases with a gapped bulk spectrum, we find a region in which the bulk spectrum is gapless if $\phi \neq 0$ or π. This is shown by the blue shaded region in Fig. 1(b); this region consists of a rectangle which is bounded by the lines $\Delta/\gamma_0 = \pm\sin\phi$ and $\mu/\gamma_0 = \pm 2\cos\phi$ and is capped by two elliptical regions on the left and right sides. There are no end modes in this region with a gapless bulk spectrum.

Next, we review the topological invariants which exist for a time-independent Hamiltonian of the form given in Eq. (8). This discussion will be useful for Sec. IV where we will study if similar topological invariants exist for a system in which the Hamiltonian varies periodically with time.

We consider a general form of h_k in Eq. (8) given by

$$h_k = a_{0,k} I + a_{1,k}\tau^x + a_{2,k}\tau^y + a_{3,k}\tau^z, \quad (11)$$

where k lies in the range $[0,\pi]$, and Hermiticity dictates that the $a_{i,k}$'s are all real functions of k. We assume that the bulk spectrum is gapped for all values of k; since the energies are given by $E_{k\pm} = a_{0,k} \pm \sqrt{a_{1,k}^2 + a_{2,k}^2 + a_{3,k}^2}$, all four of the $a_{i,k}$'s cannot vanish simultaneously at any value of k. Next, since k is the same as $-k$ for $k = 0$ and π, and the anticommutation relations imply that $f_0 f_0 = 0$ and $f_0^\dagger f_0 = -f_0 f_0^\dagger$ plus a constant (and similarly for $k = \pi$), we can assume that $a_{0,k} = a_{1,k} = a_{2,k} = 0$ for $k = 0,\pi$. Hence $a_{3,k}$ must be nonzero at $k = 0,\pi$, otherwise the bulk spectrum would be gapless. It then turns out that the quantity $\nu = \text{sgn}(a_{3,0}a_{3,\pi})$ is a topological invariant; since it can only take values ± 1, it is a Z_2-valued invariant. We find that a phase is topological

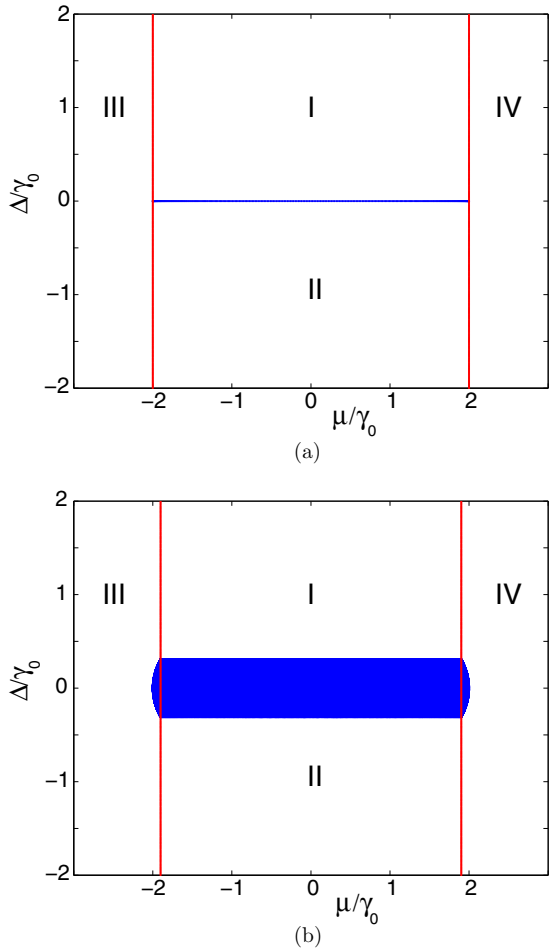

FIG. 1. Phase diagram of the model in Eq. (4) as a function of μ/γ_0 and Δ/γ_0, for (a) $\phi = 0$ and (b) $\phi = \pi/10$. Phases I and II are topological with one mode at each end of a long chain, while III and IV are nontopological with no end modes; all these phases have bulk spectra which are gapped. A blue shaded region appears in figure (b); in this region the bulk spectrum is gapless.

(with an odd number of zero energy modes at each end of a long chain) if $\nu = -1$ and is nontopological (with either no end modes or an even number of zero energy end modes) if $\nu = +1$ [43]. The symmetry class of this general model which may not have time-reversal symmetry is called class D.

If we impose time-reversal symmetry, we obtain additional constraints on the $a_{i,k}$'s and a different topological invariant. If the Hamiltonian in Eq. (11) has to be symmetric under the time-reversal transformation given in Eq. (5), we must have $a_{0,k} = a_{1,k} = 0$ for all values of k. Hence h_k only depends on two functions:

$$h_k = a_{2,k}\tau^y + a_{3,k}\tau^z. \tag{12}$$

Although Eq. (8) defines $a_{2/3,k}$ only for $0 \leqslant k \leqslant \pi$, it is convenient to analytically continue these definitions to the entire range $-\pi \leqslant k \leqslant \pi$, with $a_{2,-k} = -a_{2,k}$ and $a_{3,-k} = a_{3,k}$. Next we map h_k to a vector $\vec{V}_k = a_{2,k}\hat{y} + a_{3,k}\hat{z}$ in the y-z plane, and define the angle $\phi_k = \tan^{-1}(a_{3,k}/a_{2,k})$ made by the vector $\vec{V}_k$ with respect to the $\hat{z}$ axis. Following Ref. [44], we now define a winding number as the integral over the Brillouin zone:

$$W = \int_{-\pi}^{\pi} \frac{dk}{2\pi}\frac{d\phi_k}{dk}. \tag{13}$$

This can take any integer value and is a therefore a Z-valued topological invariant. Note that this is well defined since both $a_{2,k}$ and $a_{3,k}$ cannot simultaneously vanish at any value of k, otherwise the bulk spectrum would be gapless. A phase is topological if $W \neq 0$; such a phase will have W zero energy modes at each end of a long chain. If $W = 0$, the phase is nontopological and does not have any end modes [43]. The symmetry class of this model with time-reversal symmetry is called class BDI.

We now consider the phase diagrams shown in Fig. 1. In Fig. 1(a) we have time-reversal symmetry, and we find that the winding number W is equal to -1 in phase I, $+1$ in phase II, and zero in phases III and IV. The invariant ν is equal to -1 in phases I and II and $+1$ in phases III and IV. In Fig. 1(b) we do not have time-reversal symmetry; hence only the invariant ν is defined. We find that ν is equal to -1 in phases I and II and $+1$ in phases III and IV.

III. FLOQUET TIME EVOLUTION AND END MODES

We will now begin our study of what happens when some parameter in the Hamiltonian is varied periodically in time. In this section we will describe the numerical technique that we use to study the Floquet time evolution and to find the end modes.

We consider a general Hamiltonian which is quadratic in terms of Majorana operators. For a system with N sites, we have

$$H = \frac{i}{4}\sum_{m,n=1}^{2N} b_m M_{mn} b_n, \tag{14}$$

where M is a real antisymmetric matrix, so that iM is Hermitian. We allow M to vary periodically with time so that $M(t+T) = M(t)$. Equation (14) implies that the Heisenberg equations for the operators $b_n(t)$ are given by

$$\frac{db_m(t)}{dt} = i[H(t), b_m(t)] = \sum_{n=1}^{2N} M_{mn}(t) b_n(t). \tag{15}$$

If b denotes the column vector $(b_1, b_2, \cdots, b_{2N})^T$ (the superscript T denotes transpose), we can write the above equation as $db(t)/dt = M(t)b(t)$. The solution of this is given by

$$b(t) = U(t,0)b(0), \quad \text{where} \quad U(t,0) = \mathcal{T} e^{\int_0^t dt M(t)}, \tag{16}$$

and $\mathcal{T}$ denotes the time-ordering symbol. The time evolution operator $U(t,0)$ can be numerically computed given the form of $M(t)$. Note that $U(T,0)$ is not only a unitary matrix, it is also real and orthogonal since $M(t)$ is real.

Since $M(t)$ varies with a time period T, we will call $U(T,0)$ the Floquet operator. The eigenvalues of $U(T,0)$ are given by phases $e^{i\theta_j}$ (where the θ_j lie in the range $[-\pi,\pi]$), and they come in complex conjugate pairs if $e^{i\theta_j} \neq 1$. This is because

$U(T,0)\psi_j = e^{i\theta_j}\psi_j$ implies that $U(T,0)\psi_j^* = e^{-i\theta_j}\psi_j^*$ since $U(T,0)$ is real. For eigenvalues $e^{i\theta_j} = \pm 1$ (these eigenvalues may or may not have a degeneracy), the eigenvectors can be chosen to be real.

The Floquet operator $U(T,0)$ satisfies an additional property if the system has time-reversal symmetry. Time-reversal symmetry implies that we must have the matrix elements $M_{mn} = 0$ whenever $m - n$ is an even integer [see Eq. (5)], and $M(T - t) = M(t)$ (this imposes a restriction on the form of the driving protocol). The first property combined with the antisymmetry of $M(t)$ implies that $\Sigma^z M^T(t)\Sigma^z = M(t)$, where Σ^z is a diagonal matrix with

$$\Sigma^z_{2n-1,2n-1} = 1 \quad \text{and} \quad \Sigma^z_{2n,2n} = -1. \tag{17}$$

(Note that Σ^z is both unitary and Hermitian and satisfies $\Sigma^{z2} = I_{2N}$). We can then show that the Floquet operator $U(T,0)$ satisfies the relation

$$\Sigma^z U^T \Sigma^z = U. \tag{18}$$

Since $U^T = U^{-1}$, Eq. (18) implies that if ψ_j is an eigenvector of U with eigenvalue $e^{i\theta_j}$, $\Sigma^z\psi_j$ is an eigenvector of U with eigenvalue $e^{-i\theta_j}$. Combining this with a statement made in the previous paragraph, we see that if the eigenvalue $e^{i\theta_j}$ is nondegenerate, the vectors ψ_j^* and $\Sigma^z\psi_j$ must be identical up to a phase.

If the system has particle-hole symmetry, $U(T,0)$ satisfies the following property. Following Eq. (6), we define a particle-hole transformation matrix C which is diagonal with

$$C_{2n-1,2n-1} = (-1)^n \quad \text{and} \quad C_{2n,2n} = -(-1)^n. \tag{19}$$

(C is both unitary and Hermitian and satisfies $C^2 = I_{2N}$. Hence the eigenvalues of C are ± 1). Then particle-hole symmetry implies that

$$CUC = U. \tag{20}$$

This implies that eigenvectors of U corresponding to nondegenerate eigenvalues must necessarily be eigenvectors of C.

Following Eq. (7) we define a matrix Σ^y the only nonzero elements of which are given by

$$\Sigma^y_{2n-1,2n} = -i \quad \text{and} \quad \Sigma^y_{2n,2n-1} = i. \tag{21}$$

Note that Σ^y is Hermitian and has eigenvalues ± 1. Hence, in any state ψ, the expectation value $\psi^\dagger\Sigma^y\psi$ must lie between -1 and 1. A state with $\psi^\dagger\Sigma^y\psi = +1(-1)$ is called a particle (hole) state, respectively; this interpretation comes from the fact that the operator in Eq. (7) is related to the electron number.

We observe that the matrices C and Σ^y anticommute. This implies that if ψ is an eigenvector of C, then the expectation value $\psi^\dagger\Sigma^y\psi = 0$; this shows that such a state has equal probabilities of particles and holes.

In Sec. IV, we will consider two kinds of periodic driving of the hopping amplitude γ. In each case, we will look for eigenvectors of $U(T,0)$ which are localized near the ends of the chain. Before discussing the specific results in the next section, we will first describe our numerical method of finding the end modes and some of their general properties [21].

The most convenient way of finding eigenvectors of $U(T,0)$ which are localized at the ends is to look at the inverse participation ratio (IPR). We assume that the eigenvectors, denoted as ψ_j, are normalized so that $\sum_{m=1}^{2N} |\psi_j(m)|^2 = 1$ for each value of j; here $m = 1,2,\ldots,2N$ labels the components of the eigenvector. The IPR of an eigenvector is then defined as $I_j = \sum_{m=1}^{2N} |\psi_j(m)|^4$. If ψ_j is extended equally over all sites so that $|\psi_j(m)|^2 = 1/(2N)$ for each m, then $I_j = 1/(2N)$ and this will approach zero as $N \to \infty$. But if ψ_j is localized over a distance ξ (which is of the order of the decay length of the eigenvector and remains constant as $N \to \infty$), then we will have $|\psi_j(m)|^2 \sim 1/\xi$ in a region of length ξ and ~ 0 elsewhere; then we obtain $I_j \sim 1/\xi$ which will remain finite as $N \to \infty$. Hence, if N is sufficiently large, a plot of I_j versus j will allow us to distinguish between states which are localized and extended states. Once we find a state j for which I_j is significantly larger than $1/(2N)$, we look at a plot of the probabilities $|\psi_j(m)|^2$ versus m to see whether it is indeed an end state. Finally, we check if the form of $|\psi_j(m)|^2$ and the value of its IPR remain unchanged if N is increased. We find that the IPR of an end mode saturates to a constant value once N becomes larger than about twice its decay length ξ. We will not show a plot of the IPR versus N here since this is rather simple.

In the periodic driving protocols discussed in Sec. IV, we find that, for certain ranges of the parameter values, $U(T,0)$ has one or more pairs of eigenvectors with substantial values of the IPR. We find that each such pair corresponds to modes localized at the two ends of the system. Further, the eigenvalues of such a pair become degenerate in the limit that the system size N is much larger than the decay length ξ of the end modes. The existence of such pairs of eigenstates follows from the parity symmetry of the Hamiltonian discussed after Eq. (4) which leads to a similar symmetry of $U(T,0)$. Namely, if ψ_1 is an eigenstate of $U(T,0)$ which is localized near one end of the system, the parity transformation gives an eigenstate $\psi_2 = \mathcal{P}\psi_1$ which is localized near the other end. The eigenvalues are degenerate in the limit $N \gg \xi$; if $N \lesssim \xi$, there is tunneling between the two end modes and this breaks the degeneracy.

IV. PERIODIC DRIVING OF HOPPING AMPLITUDE

In this section we will study in detail two cases which correspond, respectively, to the magnitude and the phase of the hopping amplitude varying sinusoidally with a time period T. Namely, we will consider (i) $\gamma(t) = \gamma_0[1 + a\cos(\omega t)]$ and (ii) $\gamma(t) = \gamma_0 e^{ia\cos(\omega t)}$, where a is real and $\omega = 2\pi/T$. Physically we may think of case (i) as arising from a periodic application of pressure on the system. This would make the lattice spacing and therefore the strength of the hopping vary with time. Case (ii) can arise due to the application of electromagnetic radiation on the system. This gives rise to an electric field and therefore a vector potential which varies sinusoidally in time. The vector potential can be put into the phase of the hopping by the Peierls prescription.

Using Eqs. (4) and (14), we find that the matrix elements of $M(t)$ are given by

$$\begin{aligned}
M_{2n,2n+1} &= -M_{2n+1,2n} = \gamma_R(t) - \Delta, \\
M_{2n-1,2n+2} &= -M_{2n+2,2n-1} = -\gamma_R(t) - \Delta, \\
M_{2n-1,2n+1} &= -M_{2n+1,2n-1} = \gamma_I(t), \\
M_{2n,2n+2} &= -M_{2n+2,2n} = \gamma_I(t), \\
M_{2n-1,2n} &= -M_{2n,2n-1} = \mu,
\end{aligned} \tag{22}$$

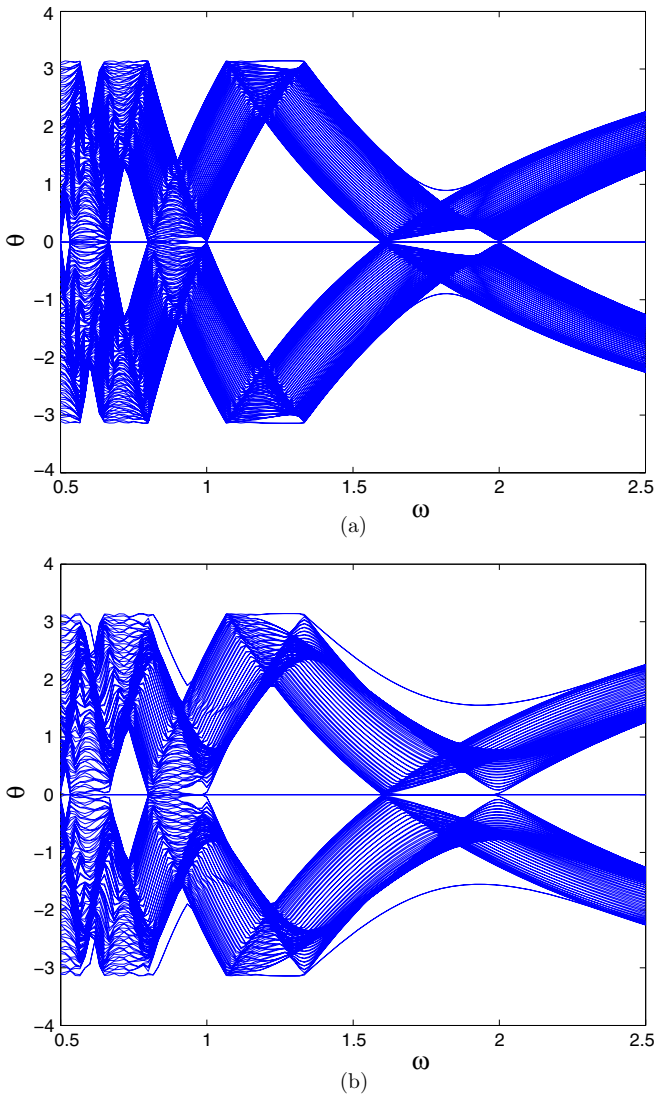

FIG. 2. Values of θ (lying in the range $[-\pi,\pi]$) vs ω, for a 200-site open chain with $\gamma_0 = 1$, $\Delta = 0.8$, $\mu = 0$, and $\gamma(t) = \gamma_0[1 + a\cos(\omega t)]$. In (a) $a = 0.5$, and in (b) $a = 1$. The isolated lines correspond to end modes: the ones with $\theta = 0$ and $\pm\pi$ are conventional end modes, while the ones with $\theta \neq 0$ or $\pm\pi$ are anomalous end modes.

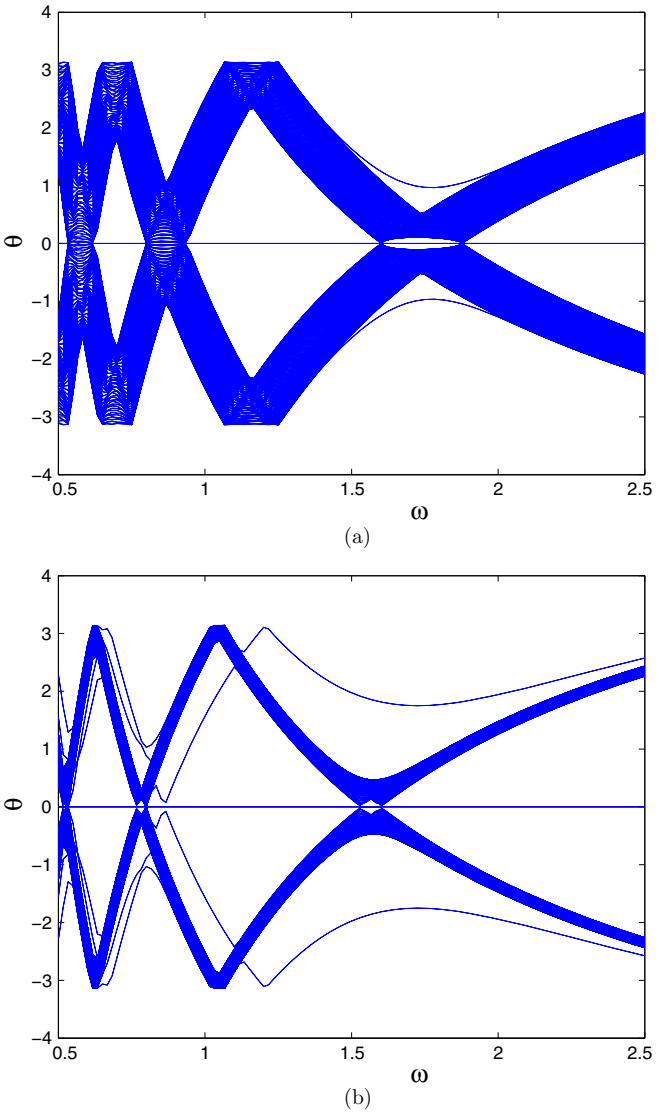

FIG. 3. Values of θ (lying in the range $[-\pi,\pi]$) vs ω, for a 200-site open chain with $\gamma_0 = 1$, $\Delta = 0.8$, $\mu = 0$, and $\gamma(t) = \gamma_0 e^{ia\cos(\omega t)}$. In (a) $a = 0.5$, and in (b) $a = 1$. The isolated lines correspond to end modes: the ones with $\theta = 0$ and $\pm\pi$ are conventional end modes, while the ones with $\theta \neq 0$ or $\pm\pi$ are anomalous end modes.

where n runs over appropriate ranges of values in the different equations, and $\gamma_R(t)$ and $\gamma_I(t)$ denote the real and imaginary parts of $\gamma(t)$. Namely, $\gamma_R = \gamma_0[1 + a\cos(\omega t)]$ and $\gamma_I = 0$ in case (i), while $\gamma_R = \gamma_0\cos[a\cos(\omega t)]$ and $\gamma_I = \gamma_0\sin[a\cos(\omega t)]$ in case (ii). We then numerically calculate the Floquet operator

$$U(T,0) = \mathcal{T}e^{\int_0^T dt M(t)}, \tag{23}$$

find all its eigenstates and eigenvalues, and use the IPR to identify the end modes as explained in Sec. III.

We will now present our numerical results. For most of our studies, we consider a 200-site open chain (hence with a 400-dimensional Hamiltonian) with $\gamma_0 = 1$, $\Delta = 0.8$, and $\mu = 0$. We begin with a quick view of the Floquet eigenvalues $e^{i\theta_j}$ of all the modes of the system. In Fig. 2 we present the values of θ_j as a function of the driving frequency ω for case (i) with $\gamma(t) = \gamma_0[1 + a\cos(\omega t)]$ for $a = 0.5$ and 1. Figure 3 shows the values of θ_j versus ω for case (ii) with $\gamma(t) = \gamma_0 e^{ia\cos(\omega t)}$ for $a = 0.5$ and 1. {The Floquet eigenvalues are sometimes written as $e^{i\theta_j} = e^{-i\epsilon_j T}$, where ϵ_j are called the quasienergies; these lie in the range $[-\pi/T,\pi/T]$. However, we will generally work with the variable θ_j rather than ϵ_j due to the simplifying feature that the range of θ_j does not depend on T.} In Figs. 2 and 3, we see some continuous bands and some isolated lines which are separated from the bands for certain ranges of ω. The bands turn out to consist of bulk modes the wave functions of which are spread throughout the system, while the isolated lines correspond to end modes the wave functions of which are localized near the two ends of the system. For some particular values of the system parameters, we have confirmed that the modes with isolated Floquet eigenvalues are end modes by

looking at the IPRs of all the eigenvectors of the Floquet operator, picking out the ones with IPRs larger by a factor of 2 or more than the remaining ones, and looking at the wave functions of these modes to check that they are localized at the ends. We find numerically that as the separation between an end mode and the bulk band decreases, the decay length of the mode from the end of the chain increases and hence its IPR decreases.

In Figs. 2(a) and 3(a), we see that the number of end modes shows several changes in the interval $1.6 \leqslant \omega \leqslant 2$ when the driving amplitude a is small. We can qualitatively understand this as follows. In the absence of driving (when $a = 0$), the parameters $\gamma_0 = 1, \Delta = 0.8$, and $\mu = 0$ place the system in the topological phase I in Fig. 1(a). An open chain then has a mode at each end with zero energy, while the bulk bands lie in the ranges $[-2,-1.6]$ and $[1.6,2]$ according to Eq. (10). Hence, periodic driving with a frequency ω can, to first order in a, produce transitions between an end mode and the bulk states if ω lies in the range $[1.6,2]$. This explains why so many changes in the end modes occur in this range of frequencies.

In Fig. 4, we show θ_j as a function of the driving amplitude a for a 200-site open chain with $\gamma_0 = 1$, $\Delta = 0.8$, $\mu = 0$, and $\omega = 1.7$. We again see some continuous bands and some isolated lines corresponding to end modes. It is clear that anomalous end modes with $\theta \neq 0$ or $\pm\pi$ appear only when a is sufficiently far from zero.

We now examine one particular case in detail to understand various aspects of the problem. We consider case (i), $\gamma(t) = \gamma_0[1 + a\cos(\omega t)]$, and we take the driving parameters to be $\omega = 1.7$ and $a = 0.5$. In Fig. 5 we show the IPRs of the 400 eigenvectors of the Floquet operator $U(T,0)$ in increasing order. We find that there are ten modes with IPRs much larger than all the others. The values of these ten IPRs and their degeneracies are given in the caption of that figure. Figure 6 shows the real and imaginary parts of all the eigenvalues of the Floquet operator; all these eigenvalues are of the form $e^{i\theta_j}$ and lie on the unit circle. We see that all the eigenvalues (except for ten) form two continuous bands, one with imaginary part positive and the other with imaginary part negative; the upper band of eigenvalues goes from $0.4458 + 0.8951i$ to $0.9971 + 0.0761i$ (namely, θ goes from 0.0762 to 1.1087) while the lower band goes from $0.4458 - 0.8951i$ to $0.9971 - 0.0761i$ (θ goes from -1.1087 to -0.0762). The remaining ten eigenvalues lie outside these bands; six of them have eigenvalue 1 (i.e., $\theta = 0$) while there are two each with eigenvalues $0.4333 \pm 0.9012i$ ($\theta = \pm 1.1226$). These ten states correspond precisely to the eigenvectors with the largest IPRs.

Looking at these ten eigenvectors, we find that they are all localized near the two ends of the chain. The four anomalous eigenvectors with eigenvalues equal to $0.4333 \pm 0.9012i$ have nonzero components $\psi_j(m)$ for both even and odd values of m at both ends (we recall that m goes from 1 to 400). However, the six eigenvectors with eigenvalues equal to 1 have nonzero components only for even values of m near the left end of the chain (i.e., near $m = 1$) and only for odd values of m near the right end of the chain (near $m = 400$). End modes with Floquet eigenvalues equal to ± 1 are sometimes called Floquet Majorana modes [6,18,21,23]; they are the time-dependent analogs of the Majorana end modes which appear in time-independent systems with zero energy [43].

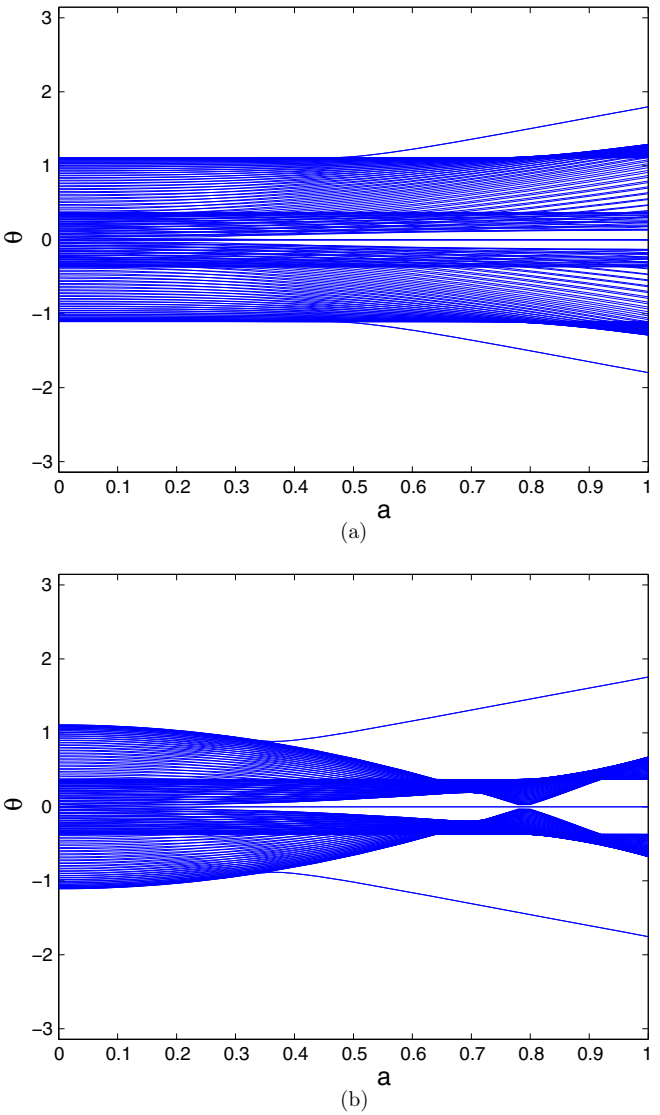

FIG. 4. Values of θ (lying in the range $[-\pi,\pi]$) vs a, for a 200-site open chain with $\gamma_0 = 1$, $\Delta = 0.8$, $\mu = 0$, and $\omega = 1.7$. In (a) $\gamma(t) = \gamma_0[1 + a\cos(\omega t)]$, and in (b) $\gamma(t) = \gamma_0 e^{ia\cos(\omega t)}$. The isolated lines correspond to end modes: the ones with $\theta = 0$ and $\pm\pi$ are conventional end modes, while the ones with $\theta \neq 0$ or $\pm\pi$ are anomalous end modes.

We find that all the ten end modes are eigenvectors of the matrix C defined in Eq. (19). Hence the expectation value of Σ^y is zero in all these modes, and each mode therefore has equal probabilities of particles and holes. (This is exactly the property that zero energy Majorana modes at the ends of an open chain have in a time-independent system [45].)

In Fig. 7, we show the probabilities $|\psi_j(m)|^2$ versus m for two eigenvectors localized at the ends, both of which have Floquet eigenvalue equal to $0.4333 + 0.9012i$. Next, we look at the Fourier transforms $\tilde{\psi}_j(k)$ of these wave functions. The Fourier transform can be defined for either odd or even numbered sites, namely, as $\tilde{\psi}_j(k) = \sum_{n=1}^{N} \psi_j(2n-1)e^{ikn}$ or $\sum_{n=1}^{N} \psi_j(2n)e^{ikn}$. For the state localized at the left end of the chain, we show $|\tilde{\psi}_j(k)|^2$ (for the even numbered sites) versus k for $0 \leqslant k \leqslant \pi$ in Fig. 8. [The figure looks identical for

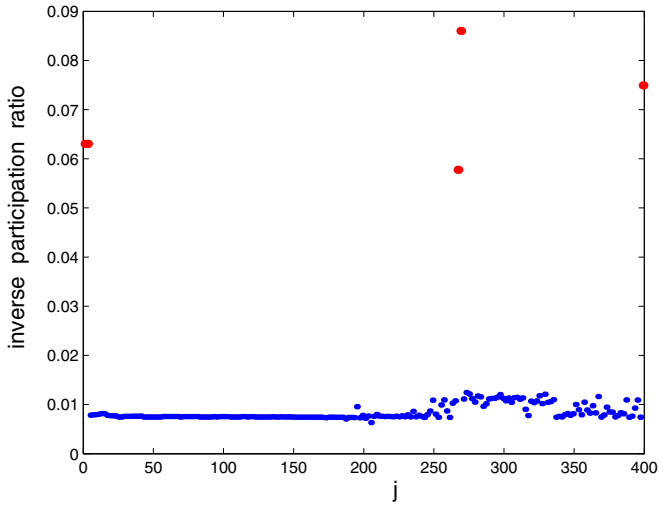

FIG. 5. IPRs of different eigenvectors of the Floquet operator for a 200-site open chain with $\gamma_0 = 1$, $\Delta = 0.8$, $\mu = 0$, $a = 0.5$, and $\omega = 1.7$. There are ten modes with large IPRs shown as large red dots; their IPR values (and their degeneracies in parentheses) are 0.0860 (two), 0.0749 (two), 0.0630 (four), and 0.0578 (two).

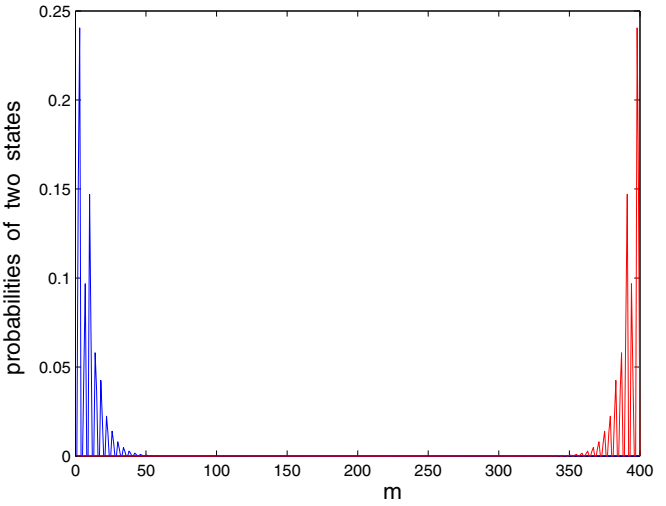

FIG. 7. Probabilities of two eigenstates of the Floquet operator which are localized at the two ends of the system; the parameter values are the same as in Fig. 5. Both states have Floquet eigenvalue equal to $0.4333 + 0.9012i$.

$-\pi \leqslant k \leqslant 0$ since $|\tilde{\psi}_j(-k)|^2 = |\tilde{\psi}_j(k)|^2$. Further, the figure looks similar, though not identical, for the Fourier transform of the odd numbered sites.] We find that the Fourier transform is peaked at $k = 0$ and π. Similar results are found for the state localized at the right end.

Similarly, in Fig. 9, we show the probabilities $|\psi_j(m)|^2$ versus m for two eigenvectors localized at the ends, both of which have Floquet eigenvalue equal to 1. For the state localized at the left end, the wave function $\psi_j(m)$ is nonzero only for even values of m; we define its Fourier transform as

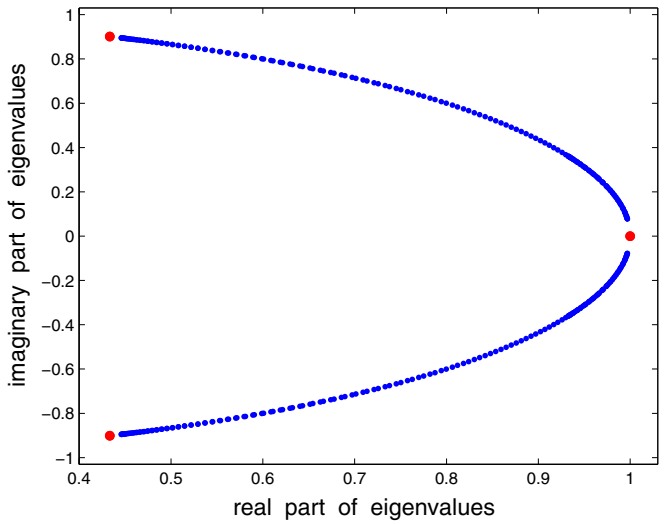

FIG. 6. Real and imaginary parts of different eigenvalues of the Floquet operator for a system with the same parameters as in Fig. 5. Ten isolated eigenvalues are visible (large red dots) corresponding to the eigenvectors with large IPRs in Fig. 5; the eigenvalues (and their degeneracies) are given by 1 (six) and $0.4333 + 0.9012i$ (two), and $0.4333 - 0.9012i$ (two). (There are no eigenvalues with real part less than 0.4333.)

$\tilde{\psi}_j(k) = \sum_{n=1}^{N} \psi_j(2n) e^{-ikn}$. Figure 10 shows $|\tilde{\psi}_j(k)|^2$ versus k for $0 \leqslant k \leqslant \pi$. We find that the Fourier transform is peaked at two values given by $k = 1.162$ and 1.979; we note that these two values add up to π. Similar results are found for the state localized at the right end.

We have checked that the results presented in Figs. 5 to 10 for the end modes (namely, the existence of ten such modes, their Floquet eigenvalues, wave functions, and the locations of the peaks of their Fourier transforms) remain unchanged if the system size is increased from 200 to, say, 300.

In Fig. 6 we see some gaps between the ends of the continuous bands of Floquet eigenvalues and the isolated Floquet eigenvalues of the end modes. We have studied how these gaps vary with the driving amplitude a. Since the

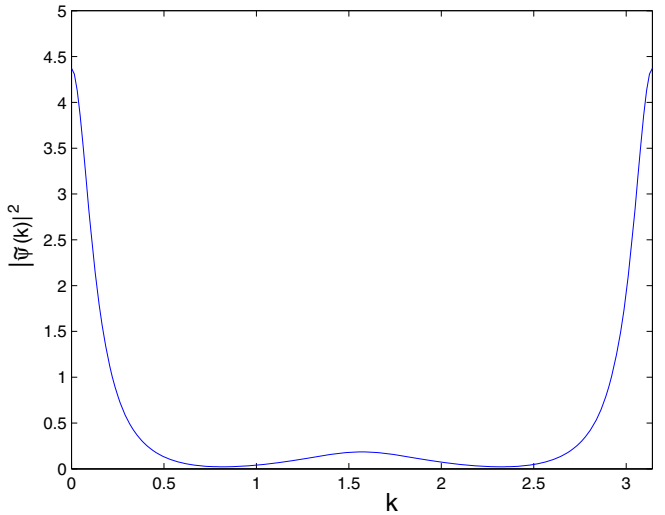

FIG. 8. $|\tilde{\psi}_j(k)|^2$ vs k for the state localized at the left end of the chain with Floquet eigenvalue equal to $0.4333 + 0.9012i$; the parameter values are the same as in Fig. 5.

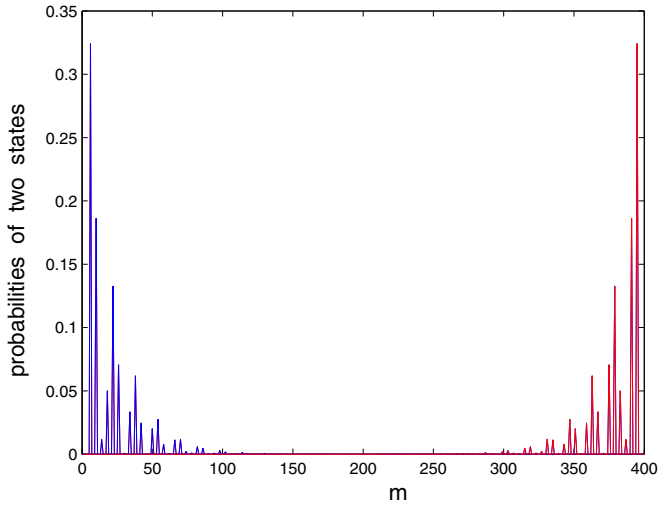

FIG. 9. Probabilities of two eigenstates of the Floquet operator which are localized at the two ends of the system; the parameter values are the same as in Fig. 5. Both states have Floquet eigenvalue equal to 1.

Floquet eigenvalues are of the form $e^{i\theta}$, we define a gap as $\Delta\theta = |\theta_1 - \theta_2|$, where θ_1 is the eigenvalue at the end of a continuous band and θ_2 is the eigenvalue for an end mode. Figure 11 shows the gap $\Delta\theta$ between the end of a continuous band and an anomalous end mode (solid blue line) and an end mode with Floquet eigenvalue 1 (red dash-dotted line). This figure implies that a significantly larger driving amplitude is required to produce the anomalous end modes compared to the end modes with Floquet eigenvalue 1.

We have studied what happens to the end modes if the chemical potential μ is not equal to zero. [This breaks the particle-hole symmetry discussed in Eqs. (6) and (19).] We have studied a 200-site open chain with $\gamma(t) = \gamma_0[1 + a\cos(\omega t)]$, where $\gamma_0 = 1$, $\Delta = 0.8$, $\omega = 1.7$, and $a = 0.5$. Upon varying μ, we discover that while the three modes at each end with Floquet eigenvalue equal to $+1$ survive up to quite large values of μ, the

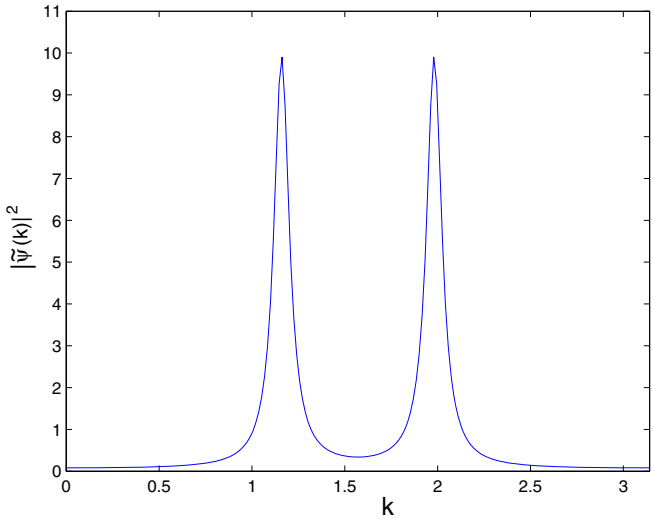

FIG. 10. $|\tilde{\psi}_j(k)|^2$ vs k for the state localized at the left end of the chain with Floquet eigenvalue equal to 1; the parameter values are the same as in Fig. 5.

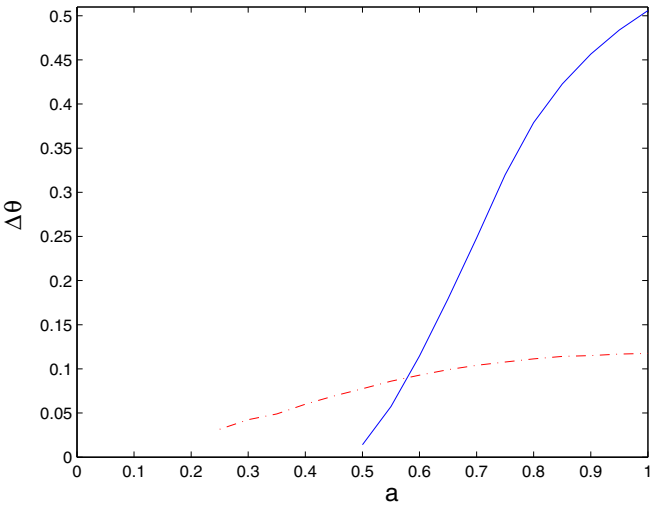

FIG. 11. Gap between the end of a continuous band of Floquet eigenvalues and the Floquet eigenvalue of an end mode vs a for a 200-site open chain with $\gamma_0 = 1, \Delta = 0.8, \mu = 0$, and $\omega = 1.7$. The solid blue line shows the gap between the end of a continuous band and an anomalous end mode (which appears for $a \gtrsim 0.5$), and the red dash-dotted line shows the gap between the end of a continuous band and an end mode with Floquet eigenvalue 1 (which appears for $a \gtrsim 0.25$).

anomalous end modes with Floquet eigenvalues far from ± 1 disappear as μ goes away from zero. To be precise, we find that the anomalous modes no longer appear when $|\mu|$ is larger than about 0.005. We can understand this small number as follows. From the earlier discussion of the Floquet eigenvalues shown in Fig. 6, we know that the gap between the Floquet eigenvalues of the anomalous end modes and the ends of the bulk bands is given by $\Delta\theta = |\cos^{-1}(0.4333) - \cos^{-1}(0.4458)| = 0.0139$. This corresponds to a quasienergy gap equal to $\Delta\epsilon = \Delta\theta/T = 0.0139(\omega/2\pi) = 0.0038$. We therefore expect that a perturbation like μ will close the gap and the anomalous end modes will disappear if μ is of the order of $\Delta\epsilon$. We see that this gives the correct order of magnitude of the value of $\mu \simeq 0.005$ beyond which there are no anomalous end modes. To conclude, the existence of an anomalous end mode is sensitively dependent on μ being close to zero, with the critical value of μ being of the order of the quasienergy gap between the anomalous mode and the nearest end of a bulk band.

Before ending this section, we briefly comment about what happens for periodic driving in case (ii), with $\gamma(t) = \gamma_0 e^{ia\cos(\omega t)}$. We have studied in detail a 200-site open chain with $\gamma_0 = 1, \Delta = 0.8, \mu = 0, \omega = 1.7$, and $a = 0.4$. We then find six end modes, three at each end. Of the three modes, two have eigenvalues $0.6216 \pm 0.7833i$ (namely, anomalous modes with $\theta = \pm 0.9000$) and one has eigenvalue 1 (i.e., $\theta = 0$). All these eigenvalues lie outside the range of the Floquet eigenvalues of the bulk modes which go from $0.6853 + 0.7283i$ to $0.9979 + 0.0649i$ and from $0.6853 - 0.7283i$ to $0.9979 - 0.0649i$ (namely, θ goes from 0.0648 to 0.8158 and from -0.8158 to -0.0648). The Fourier transforms of the anomalous end modes have peaks at $k = 0$ and π, while the Fourier transform of the end mode with Floquet eigenvalue 1 has peaks lying at $k = 1.005$ and 2.136. We also find that the expectation value of Σ^y is zero in all the end modes, implying

that each mode has equal probabilities of particles and holes. Thus all the features for this case are qualitatively similar to the results for case (i) that we have presented in Figs. 5–10. We will see in the next section that various bulk-boundary correspondences also work similarly for cases (i) and (ii) except for the winding number.

Once again, the anomalous end modes disappear when the chemical potential is moved away from zero; for the parameters given in the previous paragraph, we find that those end modes are no longer present when $|\mu|$ is 0.031 or larger.

V. BULK-BOUNDARY CORRESPONDENCE

We will now study if there are any bulk-boundary correspondences which can help us to understand some of the properties of the end modes discussed in Sec. IV. To this end, we will consider a bulk system with periodic boundary conditions.

As a specific example, we will again consider a periodic driving of the form $\gamma(t) = \gamma_0[1 + a\cos(\omega t)]$, with $\gamma_0 = 1$, $\Delta = 0.8$, $\mu = 0$, $a = 0.5$, and $\omega = 1.7$ as in Figs. 5–10. With periodic boundary conditions, the momentum k is a good quantum number; the system therefore decomposes into a sum of subsystems labeled by k. For each value of k, we have a Floquet operator which is a 2×2 matrix defined as

$$U_k = \mathcal{T} e^{-i\int_0^T dt h_k(t)},$$
$$h_k(t) = \{2\gamma_0[1 + a\cos(\omega t)]\cos k - \mu\}\tau^z + 2\Delta \sin k \tau^y. \tag{24}$$

Since each of the terms e^{-idth_k} is an SU(2) matrix (a 2×2 matrix with determinant equal to 1), U_k is also an SU(2) matrix. Further, the symmetry $h_k(T - t) = h_k(t)$ and the fact that τ^z (τ^y) is a symmetric (antisymmetric) matrix imply that $\tau^z U_k^T \tau^z = U_k$. [This is similar to the relation given in Eq. (18) for an open chain.] This implies that U_k can be written as

$$U_k = e^{i(a_{2,k}\tau^y + a_{3,k}\tau^z)}, \tag{25}$$

where $(a_{2,k}, a_{3,k})$ can be found uniquely by imposing the condition $0 < \sqrt{a_{2,k}^2 + a_{3,k}^2} < \pi$. It is possible to impose this condition as long as $U_k \neq \pm I_2$. If $U_k = \pm I_2$ for any value of k, the winding number does not exist for the following reason. We can map the operator U_k in Eq. (25) to a point on the surface of a sphere with polar angles (α, β), where $\alpha = \sqrt{a_{2,k}^2 + a_{3,k}^2}$ and $\beta = \tan^{-1}(a_{2,k}/a_{3,k})$. We get a closed curve on the sphere if we take k to go from zero to 2π; the winding number of this curve is well defined only if the curve does not pass through either the north pole or the south pole (i.e., $\alpha = 0$ or π).

If we take $(a_{2,k}, a_{3,k})$ to define the coordinates of a point in the y-z plane, we get a closed curve as k goes from zero to 2π. Figure 12 shows this curve for the parameter values given above. [We observe that the figure is symmetric under reflection about the line $a_2 = 0$; this is because of the relations $a_{2,k} = -a_{2,2\pi-k}$ and $a_{3,k} = a_{3,2\pi-k}$ which follow from Eq. (24). The figure is also symmetric under reflection about the line $a_3 = 0$; this is because we have chosen $\mu = 0$ which implies $a_{2,k} = a_{2,\pi-k}$ and $a_{3,k} = -a_{3,\pi-k}$.] We can then find the values of the two topological invariants defined in Sec. II, namely, the winding number W of the curve around the origin (0,0), and $\nu = \mathrm{sgn}(a_{3,0}a_{3,\pi})$. For the curve shown in Fig. 12 we find that $W = -3$ and $\nu = -1$. We see that $|W|$ precisely matches the number of modes at each end of the open chain with Floquet eigenvalue equal to 1, and the value of ν correctly indicates that the number of end modes with Floquet eigenvalue 1 is odd.

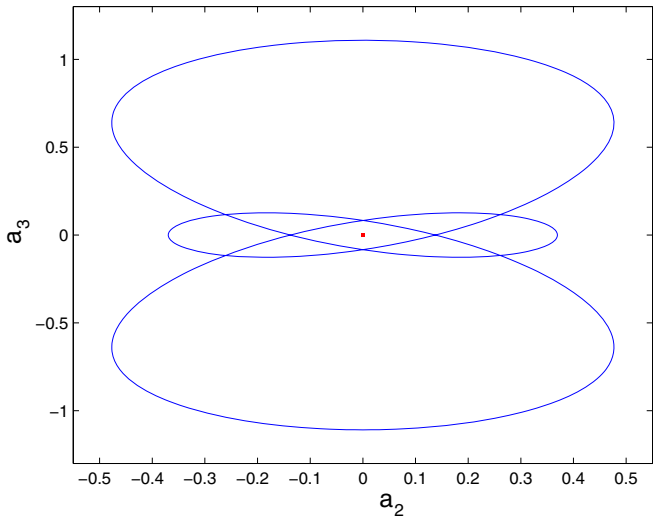

FIG. 12. Closed curves in the y-z plane defined by $(a_{2,k}, a_{3,k})$ for a system with periodic boundary conditions and the same parameter values as in Fig. 5. The winding number around the origin (0,0) (shown by a small red square) is found to be -3.

We observe that there are certain values of parameters for which $\sqrt{a_{2,k}^2 + a_{3,k}^2}$ is equal to zero or π, namely, U_k is equal to $\pm I_2$ for some value of k; the winding number and ν are both undefined in those cases. Looking at Eqs. (24) and (25), we see that this happens for all values of a if $2(\pm 2\gamma_0 - \mu)/\omega$ is an integer since U_0 or U_π is then equal to $\pm I_2$. This also happens for all values of a if $2\sqrt{\mu^2 + 4\Delta^2}/\omega$ is an integer since $U_{\pi/2}$ and $U_{3\pi/2}$ are then equal to $\pm I_2$. For the range of parameters used in Fig. 2, namely, $\gamma_0 = 1, \Delta = 0.8$, and $\mu = 0$, we see in that figure that the gap between the bulk Floquet eigenvalues and the eigenvalue at 1 (i.e., $\theta = 0$) closes at several values of ω such as $\omega = 2, 1.6, 1, 0.8, 0.667$, and 0.533; these values agree with the conditions on ω given above where the winding number is not defined.

Next, we look at the eigenvalues of $U_k = e^{\pm i\theta_k}$, where $\theta_k = \sqrt{a_{2,k}^2 + a_{3,k}^2}$. In Fig. 13, we show the real part of the Floquet eigenvalue (namely, $\cos\theta_k$) versus k for $0 \leqslant k \leqslant \pi$. (The figure looks similar for $\pi \leqslant k \leqslant 2\pi$ since $\cos\theta_{2\pi-k} = \cos\theta_k$.) We see that it has five extrema; these are at $k = 0$ and π where $\cos\theta_k = 0.4457$, $k = 1.162$ and 1.979 where $\cos\theta_k = 0.9972$, and $k = \pi/2$ where $\cos\theta_k = 0.9325$. {The value of $\cos\theta_k$ at $k = 0$ and π can be obtained easily from Eq. (24) since the coefficient of τ^y is then zero. We find that $\cos\theta_k = \cos[(2\gamma_0 - \mu)T]$, independent of the values of Δ and a.}

We note that the range of values of the Floquet eigenvalues for the bulk system with periodic boundary conditions precisely matches the range of values of the continuous band of Floquet eigenvalues for the open chain as shown in Fig. 6; this could have been anticipated. However, we now make

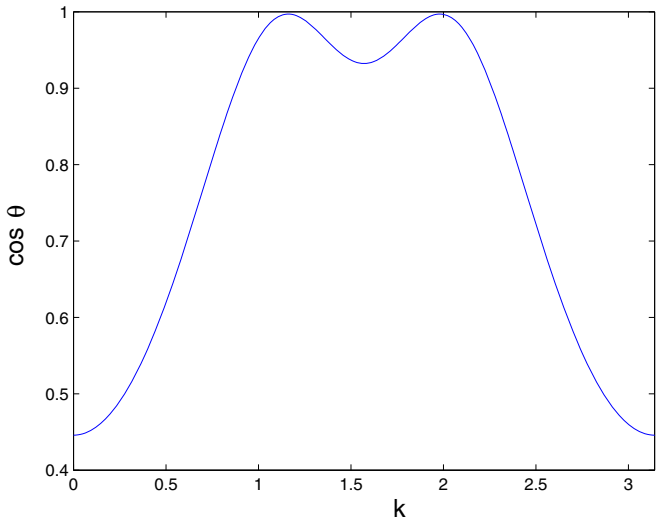

FIG. 13. Real part of Floquet eigenvalue, $\cos\theta_k$, vs k for a system with periodic boundary conditions and the same parameter values as in Fig. 5.

an additional observation. Namely, some (but not all) of the extrema of the Floquet eigenvalues of the bulk system have a close correspondence with the anomalous end modes of the open chain in two different ways. First, the values of the bulk Floquet eigenvalues at the extrema at $k = 0$ and π are close to the Floquet eigenvalues $0.4333 \pm 0.9012i$ for four of the end modes of the open chain. Second, the peaks of the Fourier transforms of these end modes lie at $k = 0$ and π. Interestingly, we also see that the values of the bulk Floquet eigenvalues at $k = 1.162$ and 1.979 are close to the Floquet eigenvalue of 1 for six of the end modes of the open chain, and the peaks of the Fourier transforms of these end modes lie at $k = 1.162$ and 1.979.

It would be useful to understand why there is such a correspondence between the extrema of the Floquet eigenvalues of the bulk system and the end modes of an open chain. We offer a speculation here. The fact of an extremum of the bulk Floquet eigenvalues near a particular value, say, $e^{i\theta'}$ at $k = k'$, means that the density of states $\rho(\theta) \equiv \int dk \delta(\theta - \theta_k)$ diverges as we approach $\theta = \theta'$. The presence of a large number of bulk states near (k',θ') perhaps makes it easy for an open chain to superpose those states to form modes which are localized at the ends. Such end modes will then naturally have a Floquet eigenvalue close to $e^{i\theta'}$ and a Fourier transform the peak of which is close to k'.

We will now comment briefly about the example of case (ii), $\gamma(t) = \gamma_0 e^{ia\cos(\omega t)}$, with $\gamma_0 = 1, \Delta = 0.8, \mu = 0, \omega = 1.7$, and $a = 0.4$ which was discussed at the end of Sec. II. In the bulk of this system, the Floquet operator for momentum k is a 2×2 matrix given by

$$\begin{aligned} U_k &= \mathcal{T} e^{-i\int_0^T dt h_k(t)}, \\ h_k(t) &= \{2\gamma_0 \cos[a\cos(\omega t)]\cos k - \mu\}\tau^z \\ &\quad + 2\gamma_0 \sin[a\cos(\omega t)]\sin k I_2 + 2\Delta \sin k \tau^y. \end{aligned} \quad (26)$$

Using arguments similar to those presented after Eq. (24), the facts that $h_k(T - t) = h_k(t)$ and I_2 commutes with both τ^y and τ^z imply that Eq. (26) can be written as

$$U_k = e^{i(a_{0,k} I_2 + a_{2,k}\tau^y + a_{3,k}\tau^z)}. \quad (27)$$

If $(a_{0,k}, a_{2,k}, a_{3,k})$ were all nonzero, they would define a closed curve in three dimensions as k goes from zero to 2π, and it would not be possible to define a winding number. However, in this problem we find that

$$a_{0,k} = -\int_0^T dt 2\gamma_0 \sin[a\cos(\omega t)]\sin k \quad (28)$$

is equal to zero for all k because the integrand changes sign under the shift $t \to t + \pi/\omega$. Hence, we only have two nonzero variables $(a_{2,k}, a_{3,k})$ as in Eq. (25) and we can therefore define a winding number W. For the parameters given above, we find that $W = 3$ which does *not* match the number of modes (namely, one) at each end of the open chain with Floquet eigenvalue 1. However, we find that $\nu = -1$, which agrees with the fact that the number of end modes with Floquet eigenvalue 1 is odd.

We now make some comments about the anomalous end modes the Fourier transforms of which have peaks at $k = 0$ and π, and we present a qualitative argument about why these modes disappear when μ moves away from zero. For $k = 0$ and π, it is easy to compute the Floquet eigenvalues of the bulk system. For case (i), $\gamma(t) = \gamma_0[1 + a\cos(\omega t)]$, we find from Eq. (24) that

$$\begin{aligned} U_0 &= \exp[-i(2\pi/\omega)(2\gamma_0 - \mu)\tau^z], \\ U_\pi &= \exp[-i(2\pi/\omega)(-2\gamma_0 - \mu)\tau^z]. \end{aligned} \quad (29)$$

If $\mu = 0$, the eigenvalues of U_0 and U_π are both equal to $e^{\pm i(4\pi/\omega)\gamma_0}$. In an open chain, the breaking of translation invariance and the degeneracy of the eigenvalues of U_0 and U_π means that the eigenvectors of U_0 and U_π can easily hybridize. This is probably the reason why they can combine to form end modes, the Floquet eigenvalues of which lie close to $e^{\pm i(4\pi/\omega)\gamma_0}$ if the driving amplitude a is small. A similar argument works for case (ii), $\gamma(t) = \gamma_0 e^{ia\cos(\omega t)}$, where Eq. (26) implies that

$$\begin{aligned} U_0 &= \exp\{-i(2\pi/\omega)[2\gamma_0 J_0(a) - \mu]\tau^z\}, \\ U_\pi &= \exp\{-i(2\pi/\omega)[-2\gamma_0 J_0(a) - \mu]\tau^z\}, \end{aligned} \quad (30)$$

where we have used the identity [46]

$$\frac{1}{2\pi}\int_0^{2\pi} d\theta \cos(a\cos\theta) = J_0(a). \quad (31)$$

Once again, if $\mu = 0$, the eigenvalues of U_0 and U_π are degenerate and equal to $e^{\pm i(4\pi/\omega)\gamma_0 J_0(a)}$, and the corresponding eigenvectors can hybridize and form end modes for an open chain. However, when μ is moved away from zero, the eigenvalues of U_0 and U_π no longer remain degenerate; this may make it difficult for their eigenvectors to hybridize and form end modes.

We end this section by pointing out some other numerical observations. All the results presented above were for cases where the frequency is of the order of or larger than the other energy scales of the system such as γ_0 and Δ and when the driving amplitude is less than or of order 1. When we move away from this regime, the results can change as follows. First, if the amplitude is much larger than 1, we sometimes find end

modes the Floquet eigenvalues of which lie far outside the range of the Floquet eigenvalues of the bulk modes. Then the Floquet eigenvalues of those end modes do not lie close to any of the extrema of the Floquet eigenvalues of the bulk modes; hence this aspect of the bulk-boundary correspondence does not work for such end modes. Second, for frequencies much smaller than γ_0 and Δ, we sometimes find end modes the Floquet eigenvalues of which lie within the range of the Floquet eigenvalues of the bulk modes. We can identify such end modes in the plot of the IPRs as in Fig. 5 but not in a plot of the Floquet eigenvalues as in Fig. 6.

VI. FLOQUET-MAGNUS EXPANSION

In this section, we will study the properties of the system when the driving frequency ω is much larger than the hopping γ_0 and the superconducting pairing Δ. In this limit we can use a Floquet-Magnus expansion in powers of $1/\omega$ to find an effective Hamiltonian [47,48].

Suppose that a Hamiltonian H varies in time with a period $T = 2\pi/\omega$. Then we can write

$$H = \sum_{n=-\infty}^{\infty} H_n e^{-in\omega t},$$
$$\text{where} \quad H_n = \frac{1}{T}\int_0^T dt\, H(t) e^{in\omega t}. \tag{32}$$

We now write the Floquet operator $U = \mathcal{T}\exp(-i\int_0^T dt\, H)$ as

$$U = e^{-iH_{\rm eff}T}, \tag{33}$$

where $H_{\rm eff}$ is called the effective Floquet Hamiltonian. Then the first three terms in the Floquet-Magnus expansion are given by [47,48]

$$H_{\rm eff} = H_0 + \sum_{n\neq 0}\frac{[H_{-n},H_n]}{2n\omega} + \sum_{n\neq 0}\frac{[[H_{-n},H_0],H_n]}{2n^2\omega^2} + \sum_{m\neq 0}\sum_{n\neq 0,m}\frac{[[H_{-m},H_{m-n}],H_n]}{3mn\omega^2}. \tag{34}$$

For a system with periodic boundary conditions, we can calculate the effective Hamiltonian in momentum space. We will use the symbols $h_{n,k}$ to denote the Fourier components of $h_k(t)$ as defined in Eq. (32) and $h_{{\rm eff},k}$ to denote the effective Hamiltonian. In the case that the hopping is periodically driven as $\gamma(t) = \gamma_0[1 + a\cos(\omega t)]$, we see from Eq. (24) that the only nonzero components $h_{n,k}$ are given by

$$h_{0,k} = [2\gamma_0\cos k - \mu]\tau^z + 2\Delta\sin k\tau^y,$$
$$h_{1,k} = h_{-1,k} = a\gamma_0\cos k\tau^z. \tag{35}$$

This implies that the term of order $1/\omega$ in $h_{{\rm eff},k}$ vanishes since $[h_{1,k},h_{-1,k}] = 0$. To order $1/\omega^2$, we obtain

$$\frac{[[h_{-1,k},h_{0,k}],h_{1,k}]}{2\omega^2} + \frac{[[h_{1,k},h_{0,k}],h_{-1,k}]}{2\omega^2} = -\frac{8a^2\gamma_0^2\Delta}{\omega^2}\cos^2 k\sin k\tau^y. \tag{36}$$

Using Eq. (34), we find that

$$h_{{\rm eff},k} = (2\gamma_0\cos k - \mu)\tau^z + 2\Delta\sin k\left(1 - \frac{4a^2\gamma_0^2}{\omega^2}\cos^2 k\right)\tau^y. \tag{37}$$

For the parameters used in Fig. 2, $\gamma_0 = 1, \Delta = 0.8$, and $\mu = 0$, we find that the Floquet operator $U_k = \exp(-ih_{{\rm eff},k}T)$ is not equal to $\pm I_2$ for any value of k if $\omega > 4$ and $4a^2/\omega^2 < 1$. We then find that the winding number is -1 and the other topological invariant $\nu = {\rm sgn}(a_{3,0}a_{3,\pi}) = -1$. We therefore expect that each end of an open chain will have one end mode with Floquet eigenvalue equal to 1 (i.e., $\theta = 0$) if ω is large enough. This agrees with what we observe in Fig. 2.

We can similarly analyze the case where $\gamma(t) = \gamma_0 e^{ia\cos(\omega t)}$. This turns out to be more complicated than the previous case in that $h_{n,k}$ is now nonzero for all values of n. Namely, using the identities [46]

$$\cos[a\cos(\omega t)] = J_0(a) + 2\sum_{m=1}^{\infty}(-1)^m J_{2m}(a)\cos(2m\omega t),$$
$$\sin[a\cos(\omega t)] = -2\sum_{m=1}^{\infty}(-1)^m J_{2m-1}(a)\cos[(2m-1)\omega t], \tag{38}$$

we find that

$$h_{0,k} = [2\gamma_0 J_0(a)\cos k - \mu]\tau^z + 2\Delta\sin k\tau^y,$$
$$h_{2m,k} = h_{-2m,k} = 2(-1)^m\gamma_0\cos k J_{2m}(a)\tau^z, \tag{39}$$
$$h_{2m-1,k} = h_{-2m+1,k} = -2(-1)^m\gamma_0\sin k J_{2m-1}(a)I_2,$$

where $m = 1,2,3,\ldots$ in the last two lines of Eqs. (39). We see that $h_{n,k} = h_{-n,k}$ for all n; hence the terms of order $1/\omega$ in $h_{{\rm eff},k}$ again vanish, and we have to go to order $1/\omega^2$. We will not discuss this case further.

VII. CONCLUSIONS

In this paper we have numerically shown that periodic driving of either the magnitude or the phase of the nearest-neighbor hopping amplitude in a one-dimensional model of electrons with p-wave superconductivity can generate end modes in a long and open chain. The end modes are of two types: some have Floquet eigenvalues $e^{i\theta}$ equal to ± 1 (i.e., $\theta = 0$ or $\pm\pi$), while the others, called anomalous, have Floquet eigenvalues different from ± 1 in complex conjugate pairs (i.e., $\theta \neq 0$ or $\pm\pi$). We observe that the anomalous end modes disappear if the chemical potential is moved sufficiently away from zero. We also find that a sufficiently large driving amplitude is required to produce the anomalous end modes. To the best of our knowledge, the anomalous end modes have not been seen earlier in models in one dimension; see, for instance, Refs. [6,17,21,33] where all the end modes are found to have Floquet eigenvalues equal to ± 1.

We have studied if there are any bulk-boundary correspondences and any topological invariants which can relate the bulk system with periodic boundary conditions and the end modes of an open chain. We find that the Z-valued winding number of the Floquet operator in the bulk matches the number of

modes at each end of a chain with Floquet eigenvalue equal to 1 if the magnitude of the hopping is periodically driven but not if the phase of the hopping is driven. In contrast to this, there is a Z_2-valued topological invariant which always agrees with the number of modes at each end with Floquet eigenvalue equal to 1 being an even or odd integer. This is in agreement with the discussion of time-reversal symmetry and topological invariants in Sec. II: the case in which the magnitude of the hopping is periodically driven is time-reversal symmetric and allows a Z-valued topological invariant, while the case in which the phase of the hopping is periodically driven is not time-reversal symmetric and only allows a Z_2-valued topological invariant. However, the anomalous end modes with Floquet eigenvalues different from ± 1 appear whether or not time-reversal symmetry is broken, and there does not seem to be any topological invariant (or any simple function of the different parameters of the system) which matches the number of such end modes. There is, however, an interesting bulk-boundary correspondence if the driving amplitude is not too large. We find that the Floquet eigenvalues of the anomalous end modes lie close to the ends of the band of Floquet eigenvalues of the bulk system (which are labeled by a momentum k). Further, the Fourier transforms of the wave functions of these end modes have peaks at values of k which match closely with the values of k where the bulk bands of Floquet eigenvalues have extrema. For instance, the Fourier transforms of the anomalous end modes have peaks at $k = 0$ and π where the Floquet eigenvalues of the bulk system have extrema. While we have presented some qualitative arguments, it would be useful to completely understand the reasons for these correspondences between the end modes and the bulk system.

We have used a Floquet-Magnus expansion to find the effective Floquet Hamiltonian in the limit that the driving frequency is much larger than the other energy scales of the system, namely, the hopping and superconducting pairing. We have found that in this limit, the number of end modes is the same as that found when there is no driving.

There has been much excitement in recent years about the possibility of detecting Majorana modes in time-independent systems of superconducting nanowires [49–53] following some theoretical proposals [54–57]. A zero-bias peak has been observed in the tunneling conductance into one end of the nanowire, and it has been suggested that this is the signature of a Majorana end mode. Our results can be tested in similar systems by applying an oscillating electric field (such as electromagnetic radiation) to the nanowire. One can study if the presence of the end modes produced by periodic driving modifies the subgap conductance peaks in some way; this has been studied in a related model in Ref. [23]. We have shown in this paper that there are two kinds of end modes: Majorana end modes with Floquet eigenvalues equal to ± 1 and anomalous end modes with Floquet eigenvalues which differ from ± 1; it would be useful to know if these contribute to conductance peaks in different ways. A question which needs to be examined in this context is how the end modes appear in the steady state of the system after the oscillatory electric field is switched on. This would require an analysis of various relaxation mechanisms which may be present in the system [5]. Finally, it would be interesting to study how the different end modes are affected by disorder in, say, the chemical potential [58–62].

ACKNOWLEDGMENTS

S.S. and S.N.S. thank Department of Science and Technology, India for Kishore Vaigyanik Protsahan Yojana Fellowships. D.S. thanks Department of Science and Technology, India for Project No. SR/S2/JCB-44/2010 for financial support.

[1] M. Z. Hasan and C. L. Kane, Rev. Mod. Phys. **82**, 3045 (2010).
[2] X.-L. Qi and S.-C. Zhang, Rev. Mod. Phys. **83**, 1057 (2011).
[3] L. Fidkowski and A. Kitaev, Phys. Rev. B **83**, 075103 (2011).
[4] T. Kitagawa, E. Berg, M. Rudner, and E. Demler, Phys. Rev. B **82**, 235114 (2010).
[5] N. H. Lindner, G. Refael, and V. Galitski, Nat. Phys. **7**, 490 (2011).
[6] L. Jiang, T. Kitagawa, J. Alicea, A. R. Akhmerov, D. Pekker, G. Refael, J. I. Cirac, E. Demler, M. D. Lukin, and P. Zoller, Phys. Rev. Lett. **106**, 220402 (2011).
[7] Z. Gu, H. A. Fertig, D. P. Arovas, and A. Auerbach, Phys. Rev. Lett. **107**, 216601 (2011).
[8] T. Kitagawa, T. Oka, A. Brataas, L. Fu, and E. Demler, Phys. Rev. B **84**, 235108 (2011).
[9] N. H. Lindner, D. L. Bergman, G. Refael, and V. Galitski, Phys. Rev. B **87**, 235131 (2013).
[10] M. Trif and Y. Tserkovnyak, Phys. Rev. Lett. **109**, 257002 (2012).
[11] A. Russomanno, A. Silva, and G. E. Santoro, Phys. Rev. Lett. **109**, 257201 (2012).
[12] V. M. Bastidas, C. Emary, G. Schaller, and T. Brandes, Phys. Rev. A **86**, 063627 (2012).
[13] V. M. Bastidas, C. Emary, B. Regler, and T. Brandes, Phys. Rev. Lett. **108**, 043003 (2012).
[14] M. Tomka, A. Polkovnikov, and V. Gritsev, Phys. Rev. Lett. **108**, 080404 (2012).
[15] A. Gomez-Leon and G. Platero, Phys. Rev. B **86**, 115318 (2012); Phys. Rev. Lett. **110**, 200403 (2013).
[16] B. Dóra, J. Cayssol, F. Simon, and R. Moessner, Phys. Rev. Lett. **108**, 056602 (2012).
[17] D. E. Liu, A. Levchenko, and H. U. Baranger, Phys. Rev. Lett. **111**, 047002 (2013).
[18] Q.-J. Tong, J.-H. An, J. Gong, H.-G. Luo, and C. H. Oh, Phys. Rev. B **87**, 201109(R) (2013).
[19] M. S. Rudner, N. H. Lindner, E. Berg, and M. Levin, Phys. Rev. X **3**, 031005 (2013).
[20] J. Cayssol, B. Dóra, F. Simon, and R. Moessner, Phys. Status Solidi RRL **7**, 101 (2013).
[21] M. Thakurathi, A. A. Patel, D. Sen, and A. Dutta, Phys. Rev. B **88**, 155133 (2013).

[22] Y. T. Katan and D. Podolsky, Phys. Rev. Lett. **110**, 016802 (2013).
[23] A. Kundu and B. Seradjeh, Phys. Rev. Lett. **111**, 136402 (2013).
[24] V. M. Bastidas, C. Emary, G. Schaller, A. Gómez-León, G. Platero, and T. Brandes, arXiv:1302.0781.
[25] T. L. Schmidt, A. Nunnenkamp, and C. Bruder, New J. Phys. **15**, 025043 (2013).
[26] A. A. Reynoso and D. Frustaglia, Phys. Rev. B **87**, 115420 (2013).
[27] C.-C. Wu, J. Sun, F.-J. Huang, Y.-D. Li, and W.-M. Liu, EPL **104**, 27004 (2013).
[28] P. M. Perez-Piskunow, G. Usaj, C. A. Balseiro, and L. E. F. Foa Torres, Phys. Rev. B **89**, 121401(R) (2014).
[29] G. Usaj, P. M. Perez-Piskunow, L. E. F. Foa Torres, and C. A. Balseiro, Phys. Rev. B **90**, 115423 (2014).
[30] P. M. Perez-Piskunow, L. E. F. Foa Torres, and G. Usaj, Phys. Rev. A **91**, 043625 (2015).
[31] M. D. Reichl and E. J. Mueller, Phys. Rev. A **89**, 063628 (2014).
[32] M. Thakurathi, K. Sengupta, and D. Sen, Phys. Rev. B **89**, 235434 (2014).
[33] J. K. Asbóth, B. Tarasinski, and P. Delplace, Phys. Rev. B **90**, 125143 (2014).
[34] R. Roy and F. Harper, Phys. Rev. B **94**, 125105 (2016).
[35] M. Thakurathi, D. Loss, and J. Klinovaja, Phys. Rev. B **95**, 155407 (2017).
[36] T. Kitagawa, M. A. Broome, A. Fedrizzi, M. S. Rudner, E. Berg, I. Kassal, A. Aspuru-Guzik, E. Demler, and A. G. White, Nat. Commun. **3**, 882 (2012).
[37] M. C. Rechtsman, J. M. Zeuner, Y. Plotnik, Y. Lumer, D. Podolsky, S. Nolte, F. Dreisow, M. Segev, and A. Szameit, Nature (London) **496**, 196 (2013).
[38] M. C. Rechtsman, Y. Plotnik, J. M. Zeuner, D. Song, Z. Chen, A. Szameit, and M. Segev, Phys. Rev. Lett. **111**, 103901 (2013).
[39] Y. Plotnik, M. C. Rechtsman, D. Song, M. Heinrich, J. M. Zeuner, S. Nolte, Y. Lumer, N. Malkova, J. Xu, A. Szameit, Z. Chen, and M. Segev, Nat. Mater. **13**, 57 (2014).
[40] L. Tarruell, D. Greif, T. Uehlinger, G. Jotzu, and T. Esslinger, Nature (London) **483**, 302 (2012).
[41] G. Jotzu, M. Messer, R. Desbuquois, M. Lebrat, T. Uehlinger, D. Greif, and T. Esslinger, Nature (London) **515**, 237 (2014).
[42] A. Kitaev, Phys. Usp. **44**, 131 (2001).
[43] W. DeGottardi, M. Thakurathi, S. Vishveshwara, and D. Sen, Phys. Rev. B **88**, 165111 (2013).
[44] Y. Niu, S. B. Chung, C.-H. Hsu, I. Mandal, S. Raghu, and S. Chakravarty, Phys. Rev. B **85**, 035110 (2012).
[45] K. Sengupta, I. Zutić, H.-J. Kwon, V. M. Yakovenko, and S. Das Sarma, Phys. Rev. B **63**, 144531 (2001).
[46] M. Abramowitz and I. A. Stegun, *Handbook of Mathematical Functions* (Dover, New York, 1972).
[47] T. Mikami, S. Kitamura, K. Yasuda, N. Tsuji, T. Oka, and H. Aoki, Phys. Rev. B **93**, 144307 (2016).
[48] M. Bukov, L. D'Alessio, and A. Polkovnikov, Adv. Phys. **64**, 139 (2015).
[49] V. Mourik, K. Zuo, S. M. Frolov, S. R. Plissard, E. P. A. M. Bakkers, and L. P. Kouwenhoven, Science **336**, 1003 (2012).
[50] M. T. Deng, C. L. Yu, G. Y. Huang, M. Larsson, P. Caroff, and H. Q. Xu, Nano Lett. **12**, 6414 (2012).
[51] L. P. Rokhinson, X. Liu, and J. K. Furdyna, Nat. Phys. **8**, 795 (2012).
[52] A. Das, Y. Ronen, Y. Most, Y. Oreg, M. Heiblum, and H. Shtrikman, Nat. Phys. **8**, 887 (2012).
[53] A. D. K. Finck, D. J. Van Harlingen, P. K. Mohseni, K. Jung, and X. Li, Phys. Rev. Lett. **110**, 126406 (2013).
[54] R. M. Lutchyn, J. D. Sau, and S. Das Sarma, Phys. Rev. Lett. **105**, 077001 (2010).
[55] Y. Oreg, G. Refael, and F. von Oppen, Phys. Rev. Lett. **105**, 177002 (2010).
[56] J. Alicea, Rep. Prog. Phys. **75**, 076501 (2012).
[57] T. D. Stanescu and S. Tewari, J. Phys.: Condens. Matter **25**, 233201 (2013).
[58] O. Motrunich, K. Damle, and D. A. Huse, Phys. Rev. B **63**, 224204 (2001).
[59] P. W. Brouwer, M. Duckheim, A. Romito, and F. von Oppen, Phys. Rev. Lett. **107**, 196804 (2011).
[60] A. M. Cook, M. M. Vazifeh, and M. Franz, Phys. Rev. B **86**, 155431 (2012).
[61] F. L. Pedrocchi, S. Chesi, S. Gangadharaiah, and D. Loss, Phys. Rev. B **86**, 205412 (2012).
[62] A. M. Lobos, R. M. Lutchyn, and S. Das Sarma, Phys. Rev. Lett. **109**, 146403 (2012).